Vol 17 No 6, June 2008
1674-1056/2008/17(06)/2097-06

Chinese Physics B

© 2008 Chin. Phys. Soc.
and IOP Publishing Ltd

Close coupling calculations for excitation partial cross sections in Ne–HF collisions*

Yu Chun-Ri(余春日)†

School of Physics & Electric Engineering, Anqing Teachers College, Anqing 246133, China

(Received 24 September 2007; revised manuscript received 1 October 2007)

This paper reports that an exact quantum close coupling calculation is carried out for rotational excitation in Ne–HF collisions on the available anisotropic potential. Partial cross sections are obtained separately at the incident energies of 48.35, 75, 120 and 150 meV. The reliability of the results is demonstrated by comparison with previously published theoretical findings. Based on the calculations, the effect of the potential energy surface on the excitation partial cross sections is discussed in detail.

Keywords: close coupling calculation, excitation partial cross section, Ne–HF collision
PACC: 3440, 3430, 3450E

1. Introduction

Inelastic vibrational–rotational excitation in atom–diatomic molecule systems can provide a great deal of information for reference in practical processes, such as intramolecular vibrational predissociation, gas phase relaxation and predicting the laser action.[1−5] Rare-gas-hydrogen-halide complexes have served as prototypes for studying both weakly intermolecular interaction and collision dynamics. Considerable attention has been paid, both by theory and experiment, to the interactions and scattering of the complexes.[6−13] In particular High-resolution infrared spectra of Ne–HF were first reported by Nesbitt *et al.*[14] The complex shows interesting dynamical features such as J-dependent predissociation rates, which allowed the determination of a rigorous upper limit to the binding energy. Microwave spectra of Ne–HF have also been observed.[15] In subsequent studies, the spectroscopy of the deuterated counterpart Ne-DF was investigated.[16] In parallel with the experimental efforts, O'Neil *et al*[17] constructed an *ab initio* potential energy surface (PES) using the correlated electron pair approximation (CEPA) and used it in rovibrational calculations. The agreement between the experimental results on Ne–HF and the theoretical predictions was reasonable. Lovejoy and Nesbitt[16] subsequently adjusted the CEPA potential to reproduce their observed spectra for Ne-DF, and the resulting potential also gave a good account of the spectra of Ne–HF. However, little of the collision dynamics of Ne–HF system has been reported.[18] The aim of this paper is to obtain the effect of the PES for the Ne–HF complex on the inelastic partial cross sections (PCSs). The paper is organized as follows. In next section, we briefly review the close coupling approach used in our calculation, a parametrized functional form of the CEPA potential for the Ne–HF complex in its ground electronic state is then presented. Subsequently, we report the calculated results for the rotational excitation PCSs on the above PES and the comparison with previous theoretical findings. Conclusions constitute the closing section.

2. Theoretical calculations

2.1. The close-coupling approach

The Hamiltonian of the scattering system between an atom and a diatomic molecule can be expressed as[19]

$$H = -\frac{\hbar^2}{2\mu_{A,BC}}\nabla_R^2 - \frac{\hbar^2}{2\mu_{BC}}\nabla_r^2 + V(\hat{\boldsymbol{R}}, \hat{\boldsymbol{r}}, \cos\theta), \quad (1)$$

where $\mu_{A,BC}$ and μ_{BC} are the total reduced mass of the scattering system and the reduced mass of the di-

*Project supported by the Natural Science Foundation of the Anhui Education Bureau of China and the National Natural Science Foundation of China (Grant No 10676025).
†E-mail: cryu2@126.com

atomic molecule respectively, and cos $\theta = \hat{\boldsymbol{R}} \cdot \hat{\boldsymbol{r}}$, The total wave-function of the system has the following form

$$\psi_\alpha(\boldsymbol{R},\boldsymbol{r}) = \frac{1}{K_{n_\alpha j_\alpha} R} \sum_{n_\gamma j_\gamma l_r J} g^J_{n_r j_r l_r, n_a j_a M_a}(R) \times \phi_{n_r j_r}(r) Y^{l_r j_r}_{J M_\alpha}(\hat{\boldsymbol{R}}, \hat{\boldsymbol{r}}). \quad (2)$$

Where $g(R)$ is the radial wavefunction of the relative motion between the atom and diatom, $\phi\ (r)$ is the radial part of the ro-vibrational wave function for the diatomic molecule, α is the incident channel and γ is the other possible channel, n is the vibrational quantum number, J is the quantum number of total angular momentum of the system, and l_γ and j_γ are the orbital quantum number of the incident atom and the rotational quantum number of the molecule in γ channel, respectively. The total wavefunction $\psi_\alpha(\boldsymbol{R},\boldsymbol{r})$ is given by the solution of the Schrödinger equation

$$(H - E)\psi_\alpha(\boldsymbol{R},\boldsymbol{r}) = 0. \quad (3)$$

Substituting Eqs.(1) and (2) into Eq.(3), we have

$$\left(\frac{\mathrm{d}^2}{\mathrm{d}R^2} - \frac{l_\beta(l_\beta+1)}{R^2} + k^2_{n_\beta j_\beta}\right) g^J_{n_\beta j_\beta l_\beta, n_a j_a M_a}(R) = \frac{2\mu_{A,BC}}{\hbar^2} \sum_{n_r j_r l_r} V^J_{n_\beta j_\beta l_\beta, n_\gamma j_\gamma l_\gamma}(R) \times g^J_{n_\beta j_\beta l_\beta, n_a j_a M_a}(R). \quad (4)$$

Equation (4) is the close coupling equation in atom-diatomic collisions.

2.2. Interaction potential for Ne–HF

Using the CEPA wavefunction and counterpoise correction, O'Neil *et al*[17] performed the Ne–HF interaction energies at a series of linear and nonlinear geometries. The HF internuclear distance is fixed at the experimental value of 0.0917 nm in all calculations. Figure 1 displays how the calculated interaction energy varies as neon recedes from the HF centre of mass in different configurations. The characteristic parameters of the PES are shown in Table 1. Here, θ is the Jacobian angle (0° corresponds to a linear Ne-H-F geometry), R_m is the equilibrium distance between Ne and HF centre of mass, V_m is the interaction energy at $R = R_\mathrm{m}$, R_0 denotes the position where the interaction energy is zero.

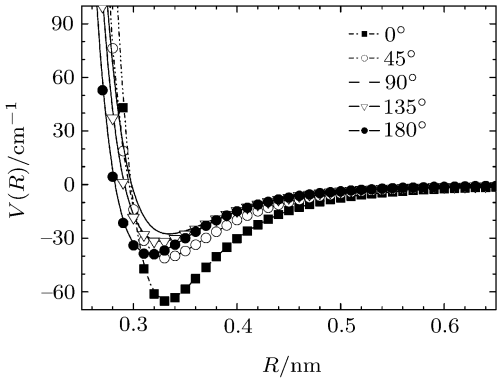


Fig.1. Section of the Ne–HF potential energy surface associated with different Jacobian angles.

Table 1. The characteristic parameters of the PES for Ne–HF complex at selected directions.

$\theta/(^\circ)$	0	45	90	135	180
$V_\mathrm{m}/\mathrm{cm}^{-1}$	–65.103	–41.081	–27.865	–32.113	–39.155
R_m/nm	0.3308	0.3305	0.3336	0.3257	0.3155
R_0/nm	0.2967	0.2950	0.2973	0.2904	0.2813

From the PES we can see that the global minimum has an energy of –65.103 cm^{-1} at R=0.3308 nm in the Ne-H-F linear configuration (θ=0°), a secondary minimum has an energy of –39.155 cm^{-1} at R=0.3155 nm in the Ne-F-H linear configuration (θ=180°), and an intervening saddle point of $-27.865\,\mathrm{cm}^{-1}$ at $R = 0.3336$ nm in the T-shaped configuration (θ=90°).

In preparation for a quantum dynamical calculation, we expand the PES of Ne–HF complex in Legendre polynomials as

$$V(R,r,\theta) = \sum_\lambda V_\lambda(R,r) P_\lambda(\cos\theta), \quad (5)$$

where R, r and θ are the conventional Jacobian coordinates of the Ne position vector $\boldsymbol{R}$ with the origin at the HF centre of mass, R represents the length of vector R, and θ the angle this vector makes with the HF molecule, taking as θ=0° the linear Ne-H-F configuration, r is the bond length of HF (fixed at its equilibrium value of 0.0917 nm). Each radial coefficient $V_\lambda(R)$ of the Legendre expansion Eq.(5) can be expressed employing the Maitland–Smith potential[20]

$$V_\lambda(R) = V_\mathrm{m}[6/(n-6)x^{-n} - n/(n-6)x^{-6}], \quad (6)$$

where $x = R/R_\mathrm{m}$, n=β+ $\gamma\ (R/R_\mathrm{m} - 1)$ and $V_\mathrm{m} = V(R_\mathrm{m})$. The parameters of the Maitland–Smith potential for λ=0–4 are shown in Table 2.

Table 2. The fitted parameters of the Maitland–Smith potential for Ne–HF system.

Coefficient	V_0	V_1	V_2	V_3	V_4
V_m/cm^{-1}	–33.9508	–8.4269	–15.6267	–6.4274	–2.6228
R_m/nm	0.3301	0.3399	0.3148	0.3388	0.3347
β	13.2402	17.1332	15.2049	18.2473	20.0821
γ	9.3170	22.320	18.3614	23.2438	32.8652

In order to demonstrate the reliability of the results, we make a comparison with the coefficients of a Legendre expansion of V (R, θ) at R=0.3174 nm[14] in Table 3. The largest two terms are V_0 and V_2, corresponding to a mostly isotropic well modulated by a double angular minimum, with λ =1, 3, 4 etc., contributions at the –5 cm^{-1} level or less. Compared with the results of the literature Ref.[14], the relative errors of the V_0 and V_2 are 0.30% and 0.61%, respectively. The agreement confirms the rationality of above results.

Table 3. Comparison of the coefficients of a Legendre expansion of V (R, θ) at R=0.3174 nm for the Maitland–Smith potential of the Ne–HF system.

Coefficient (R=0.3174 nm)	V_0/cm^{-1}	V_1/cm^{-1}	V_2/cm^{-1}	V_3/cm^{-1}	V_4/cm^{-1}
The value in the literature[14]	–31.418	–5.823	–15.485	–3.429	–1.934
The calculated value in this paper	–31.324	–5.647	–15.580	–4.178	–2.023
The relative error/%	0.30	3.00	0.61	21.80	4.60

3. Results and discussion

By solving the close-coupling differential equation, we have obtained the PCSs for the rotational excitation on the above Maitland–Smith potential. The calculations are performed separately at the incident energies of 48.35, 75, 120 and 150 meV. 175 coupled channels for 7 rational states are included for the computed partial waves. The convergence is demonstrated with up to 200 coupled channels test calculations for selected partial waves. We assume that the partial wave is convergent when the value of PCS reaches $10^{-4}a_0^2$, where a_0 is the Born radius.

In order to understand better the collision energy transfer process, we inspect the contribution of each inelastic partial wave to the total inelastic PCS. In Figs.2 and 3 we show respectively the variations of the total inelastic PCS and state-to-state excitation PCS with the increase of the quantum number J of total angular momentum at the collision energy of 150 meV. The typical character of the curves is that there are two peaks for the total inelastic PCS and the lower rotational transitions of j=0→ j'=1, 2, but only one peak for the higher rotational transitions of j=0→ j'= 3, 4, 5, 6. Similar character is seen for He–HF, He–HCl and He–HBr scattering.[9,10,12] They result from the interference of quantum mechanical waves, which are associated with different classical trajectories that lead to the same angular momentum transfer. Since the molecule is initially in ground rotational state j=0, the quantum number J of total angular momentum equals the quantum number l of orbital angular momentum of the incident channel, and these plots also represent PCSs as functions of the quantum number l of initial orbital angular momentum. Classically, impact parameter can be associated with a given l using the relation[21]

$$b_l \sim \hbar l/P = \hbar l/\sqrt{2\mu E}, \tag{7}$$

where μ is the reduced mass of the Ne–HF system, E is the collision energy.

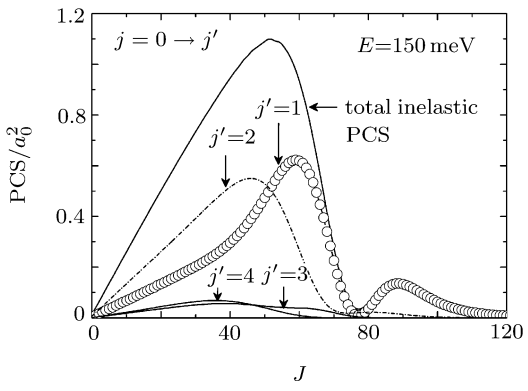


Fig.2. The total inelastic and state-to-state PCSs from the initial j=0 to final state j' as functions of total angular momentum J at the incident energy of 150 meV.

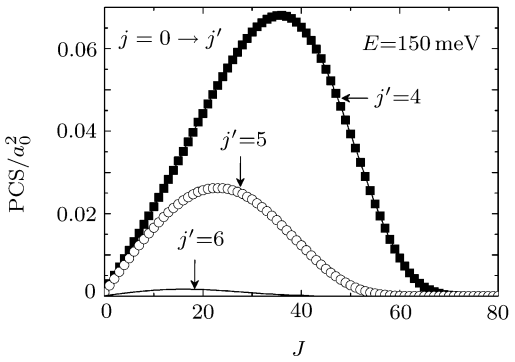


Fig.3. The state-to-state PCSs from the initial j=0 to final state j' as functions of total angular momentum J at the incident energy of 150 meV.

In terms of Eq.(7), the calculated impact parameters corresponding to the characteristic value J of the total inelastic PCS are as follows: b_{51}=0.1903 nm, b_{77}=0.2874 nm, b_{89}=0.3322 nm.

From Table 4 we notice that b_{77} and b_{89} corresponding to the minimum and tail maximum in the total inelastic PCS are almost the locations of the short-range repulsive and long-range attractive well of the PES, respectively. And b_{51} corresponding to the main peak is less than b_{77}. These mean that orbital angular momenta from 0 to 77 correspond to the scatterings in the hard repulsive parts of the potential, those from 77 to 89 correspond to the collisions in the region where both the short-range attractive and short-range repulsive parts of the potential contribute to the PCSs, For $l > 89$, the scattering is determined by the long-range attractive part of the potential.

Based on the above argument, we suggest a reasonable interpretation for the behaviour of the collision dynamics shown in Figs.2 and 3 as follows. First of all, the total inelastic PCS comes mainly from the transitions of $j = 0 \rightarrow j'$=1, 2, and the contribution of the former to the tail maximum at high J is predominant over that of the latter; yet the contribution of the two transitions to the main peak is almost the same. It is understandable that the PCS coming from the transition of $j = 0 \rightarrow j'$=1 is determined by the long-range attractive and anisotropic short-range parts of the PES. However, for the transition of $j = 0 \rightarrow j'$=2, the contribution of the long-range attractive part of the PES to the PCS is extremely small. The PCSs coming from the transitions of $j = 0 \rightarrow j' \geq 3$ are determined almost by the anisotropic short-range part of the PES. Secondly, the main peaks of the state-to-state excitation PCS lie between J=0 and J=77, and the contribution of the lower excitation transitions of $j = 0 \rightarrow j'$=1, 2 to the main peak of the total inelastic PCS is much larger than the higher the state-to-state excitation transitions, which correspond to the hard repulsive part of the potential. This demonstrates that J=0 through 77 is very efficient in exciting HF molecule from j=0 to j'=1, 2. As for the J values of 77 to 89, the short-range attractive well on the F side of the potential also contributes a considerable quantity of PCSs, except for the contributions from repulsive part. When J arrives at 77, the net contribution reaches its minimum.

Figure 4 shows the PCSs for the same rotational transitions as in Figs.2 and 3 but at the collision energy of 48.35 meV. It is very obvious that the behaviour of the PCSs as a function of the total angular momentum number J is similar to that in the case of E=150 meV as shown in Figs.2 and 3. For example, although the positions of the two peaks and of the minimum in the inelastic transition $j = 0 \rightarrow j'$=1 are different in the two cases, but they correspond to almost the same impact parameters,

$$b_{28}=0.1841\,\text{nm},\ b_{44}=0.2892\,\text{nm},\ b_{51}=0.3352\,\text{nm}\ \text{ for }\ E=48.35\,\text{meV};$$
$$b_{59}=0.2202\,\text{nm},\ b_{77}=0.2874\,\text{nm},\ b_{89}=0.3322\,\text{nm}\ \text{ for }\ E=150\,\text{meV}.$$

This means that the collision parameters sample the same portions of the PES. As the collision energy increases, the Ne atom penetrates easily into the potential, so the values of impact parameters related to the main peaks increase slightly. In addition, we see again that the long-range attractive well makes a significant contribution to the tail maximum for the lower Δj inelastic transitions, whereas it does not exist for the higher inelastic transitions, as seen from Figs.2 and 3. Thus, we consider the interpretation for the collision dynamics of E=48.35 meV in Fig.4 to be similar to that at E=150 meV in Figs.2 and 3.

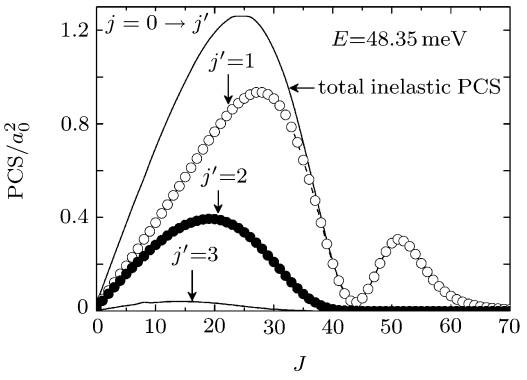


Fig.4. The total inelastic and state-to-state PCSs from the initial j=0 to final state j' as functions of total angular momentum J at the incident energy of 48.35 meV.

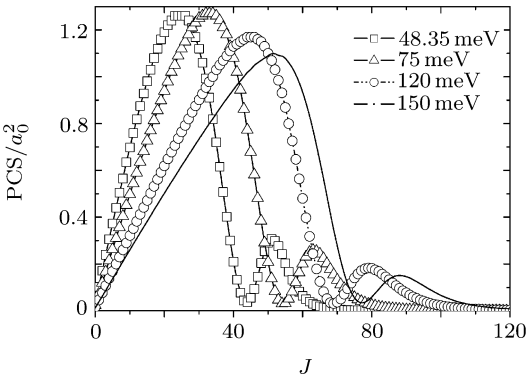


Fig.5. The total inelastic PCSs as functions of total angular momentum J at the collision energies: 48.35, 75, 120 and 150 meV. The HF molecule is initially in the state of j=0.

Figure 5 displays the variation of the total inelastic PCS for Ne–HF collision with the increase of total angular quantum number J at different collision energies. The characteristic value J and impact parameters corresponding to the two peaks and the minimum of each inelastic PCS are shown in Table 4. From Fig.5 and Table 4, once again we can see that although the positions of the two peaks and the minimum in the inelastic PCS are different in the four cases, they correspond to almost the same impact parameters. For instance, for the tail maxima of the inelastic PCSs,

$$B_{51}=0.3352\,\text{nm} \quad \text{for} \quad E=48.35\,\text{meV}, \quad b_{63}=0.3325\,\text{nm} \quad \text{for} \quad E=75\,\text{meV},$$
$$B_{79}=0.3296\,\text{nm} \quad \text{for} \quad E=120\,\text{meV}, \quad b_{89}=0.3322\,\text{nm} \quad \text{for} \quad E=150\,\text{meV}.$$

Table 4. The characteristic value J and impact parameters corresponding to the two peaks and the minimum of each inelastic PCS at different collision energies for Ne–HF complex.

48.35 meV	main peak	minimum	tail max	75 meV	main peak	minimum	tail max
$l(J)$	24	44	51	$l(J)$	33	54	63
b_l/nm	0.1578	0.2892	0.3352	b_l/nm	0.1742	0.2850	0.3325
120 meV	main peak	minimum	tail max	150 meV	main peak	minimum	tail max
$l(J)$	45	69	79	$l(J)$	51	77	89
b_l/nm	0.1878	0.2879	0.3296	b_l/nm	0.1903	0.2874	0.3322

4. Conclusions

According to the discussion above, the following conclusions can be drawn:

(1) The long-range attractive well of the PES makes the significant contribution to the PCSs, especially the tail maximum for $j=0\rightarrow j'$=1 transitions, whereas no contribution is for the $j'\geq 3$ inelastic transitions.

(2) The short-range (the repulsive and attractive) interaction makes the significant contribution to PCSs, especially the main peak for $j=0\rightarrow j'$=1, 2. As for the transitions of $j'\geq 3$, the short-range interaction plays a key role in the inelastic excitation.

(3) Although the positions of the maxima and minima of the inelastic PCSs are different at different collision energies considered here, they correspond to almost the same impact parameters.

We believe that this work can provide some information for further scattering experiments and theoretical study[22−27] of weakly interacting molecules.

References

[1] Sun G H, Yang X D, Zhu J and Wang C X 2002 *Chin. Phys.* **11** 910

[2] Chu T S, Xie T X and Han K L 2004 *J. Chem. Phys.***121** 9352

[3] Isamu M and Koichi M T Y 2005 *J. Mol. Spect.* **233** 77

[4] Linghu R F and Xu M 2006 *J. At. Mol. Phys.* **23** 1105 (in Chinese)

[5] Wang R K, Linghu R F and Yang X D 2007 *Acta Phys. Sin.* **56** 2067 (in Chinese)

[6] Held W D, Piper E, Ringer G and Toennies J P 1980 *Chem. Phys. Lett.* **75** 260

[7] Murdachaew G, Szalewicz K, Jiang H and Bacic Z 2004 *J. Chem. Phys.* **121** 11839

[8] Lotrich V F, Wormer P E S and Avoird A 2004 *J. Chem. Phys.* **120** 93

[9] Yu C R, Huang S Z, Feng E Y, Wang R K, Cheng X L and Yang X D 2006 *Acta Phys. Sin.* **55** 2215 (in Chinese)

[10] Yu C R, Feng E Y, Wang R K and Yang X D 2006 *Chin. Phys.* **15** 2571

[11] Yu C R, Wang R K, Cheng X L and Yang X D 2007 *Acta Phys. Sin.* **56** 2577 (in Chinese)

[12] Yu C R, Cheng X L and Yang X D 2007 *Chin. Phys. Lett.* **24** 1234

[13] Yu C R, Feng E Y, Cheng X L and Yang X D 2007 *Acta Phys. Sin.* **56** 4441 (in Chinese)

[14] Nesbitt D J, Lovejoy C M, Lindeman T G, ONeil S V and Clary D C 1989 *J. Chem. Phys.* **91** 722

[15] Fraser G T and Suenram R D 1990 *J. Mol. Spectrosc.* **140** 141

[16] Lovejoy C M and Nesbitt D J 1991 *J. Chem. Phys.* **94** 208

[17] O'Neil S V, Nesbitt D J, Rosmus P, Werner H J and Clary D C 1989 *J. Chem. Phys.* **91** 711

[18] Chapman W B, Weida M J and Nesbitt D J 1997 *J. Chem. Phys.* **106** 2248

[19] Choi B H and Tang K T 1975 *J. Chem. Phys.* **63** 1775

[20] Maitland G C and Smith E B 1973 *Chem. Phys. Lett.* **22** 443

[21] Bransden B H 1983 *Atomic Collision Theory* (Boston, MA: Benjamin–Cummings) p12

[22] Yu C R, Shi S H, Wang R K and Yang X D 2007 *Chin. Phys.* **16** (Accepted)

[23] Sun J F, Zhang J C and Wang J M 2006 *Chin. Phys.* **15** 531

[24] Shi D H, Sun J F, Zhu Z L and Liu R F 2006 *Acta Phys. Sin.* **55** 2228 (in Chinese)

[25] Sun G H and Yang X D 2002 *Acta Phys. Sin.* **51** 506 (in Chinese)

[26] Hu B T, Chen C H, Song Y S and Gu J G 2007 *Chin. Phys.* **16** 1285

[27] Yu C R, Huang S Z, Shi S H, Cheng X L and Yang X D 2007 *Acta Phys. Sin.* **56** (Accepted, in Chinese)